CANCER

Intratumoral nanoplexed poly I:C BO-112 in combination with systemic anti–PD-1 for patients with anti–PD-1–refractory tumors

Iván Márquez-Rodas[1]*, Federico Longo[2], Maria E. Rodriguez-Ruiz[3], Antonio Calles[1], Santiago Ponce[4], Maria Jove[5], Belén Rubio-Viqueira[6], Jose Luis Perez-Gracia[7], Ana Gómez-Rueda[2], Sara López-Tarruella[1], Mariano Ponz-Sarvise[3], Rosa Álvarez[1], Ainara Soria-Rivas[2], Enrique de Miguel[8], Rocío Ramos-Medina[1], Eduardo Castañon[7], Pablo Gajate[2], Cayetano Sempere-Ortega[9], Elisabeth Jiménez-Aguilar[4], M. Angela Aznar[3], Aitana Calvo[1], Pedro P. Lopez-Casas[10], Salvador Martín-Algarra[7], Miguel Martín[1], Dominique Tersago[10†], Marisol Quintero[10†], Ignacio Melero[3]

Intratumoral therapies, especially Toll-like receptor agonists, can trigger both the innate and adaptive immune systems. BO-112 is a nanoplexed form of polyinosinic:polycytidylic acid (poly I:C) that induces local and systemic immunotherapeutic effects in mouse models. In a multicenter phase 1 clinical trial, repeated intratumoral administrations of BO-112 induced an increase in tumor cell necrosis and apoptosis, as well as augmented immune reactivity according to gene expression profiling. The first three cohorts receiving BO-112 as a monotherapy resulted in a recommended dose of 1 mg that could be safely repeated. Two grade 3 to 4 adverse reactions in the form of reversible thrombocytopenia were reported. In a fourth cohort of 28 patients with tumors that had primary resistance to anti–programmed cell death protein–1 (PD-1), the combination of intratumoral BO-112 with nivolumab or pembrolizumab was also well tolerated, and 3 patients (2 with melanoma and 1 with renal cell carcinoma) achieved partial responses, with 10 more patients having stable disease at 8 to 12 weeks. Thus, local BO-112 combined with a systemic anti–PD-1 agent might be a strategy to revert anti–PD-1 resistance.

INTRODUCTION

Understanding the mechanisms behind the different patterns of immune recognition of tumors is key to reverse resistance to anti–programmed cell death protein 1 (PD-1) blockade in patients with cancer. Agents with the ability to elicit innate and adaptive immune responses could exert therapeutic effects against both local and distant noninjected tumors and are among the current strategies being explored (*1*). An important advantage of the local administration approach is that it often lessens toxicity through reduced systemic exposure (*2*). Although randomized clinical trial results are pending, early studies with different intratumoral treatments, ranging from cytokines and oncolytic viruses (*3*) to synthetic nucleotides (*4*) or analogs of bacterial products (*5*), suggest potential synergistic effects in combination with anti–PD-1 therapy with no additional or unexpected toxicities. Conceptually, the injected tumor lesion would expose tumor antigens shared by the injected tumor and distant metastatic lesions, leading to a presentation of tumor antigens by professional antigen-presenting cells (*6*). The most clinically advanced intratumoral agent of this kind is an attenuated oncolytic herpes simplex virus vector that encodes for GM-CSF (granulocyte-macrophage colony-stimulating factor) (T-VEC) and is used in combination with systemic pembrolizumab for the treatment of melanoma (*3*).

The immune system has evolved receptors and pathways to be alerted by the presence of pathogen-associated molecular patterns such as double-stranded mRNA, which denotes viral infection (*7*). BO-112 is a synthetic doubled-stranded, noncoding RNA (dsRNA) polyinosinic:polycytidylic acid (poly I:C), nanoplexed with the cationic carrier polyethylenimine (PEI). The latter facilitates the delivery into the cells and protects poly I:C from nucleases. BO-112 is formulated for optimal functionality and reproducibility regarding particle size and ratio of poly I:C to PEI. Poly I:C acts as a chemical analog of dsRNA that mimics viral RNAs and is sensed by Toll-like receptor 3 (TLR3) in endosomes and by melanoma differentiation–associated protein 5 (MDA5) in the cytosol to set in motion the innate immunity primarily driven by induction of type I interferons (IFNs) (*8*). Several TLR3 agonists have been or are undergoing clinical development for intratumoral administration including poly I:C stabilized with polylysine and carboxymethylcellulose (poly ICLC) and poly ICLC combined with FMS-like tyrosine kinase 3 ligand (Flt3l) (*4*, *9*). The first preclinical and clinical studies of poly I:C–related compounds administered systemically were conducted as early as 1985 (*10*), with a good safety record, although the limited antitumor activity redirected the clinical development of these compounds toward other conditions, such as chronic viral infections (*11*) and chronic fatigue syndrome (*12*). The main indications for local use were related to the performance of poly I:C–related compounds as vaccine adjuvants (*13*), with a good intradermal safety profile documented in healthy volunteers (*14*).

[1]Medical Oncology Department, Instituto de Investigación Sanitaria Gregorio Marañón and CIBERONC, Madrid 28007, Spain. [2]Medical Oncology Department, Hospital Ramón y Cajal, IRYCIS and CIBERONC, Madrid28034, Spain. [3]CIMA and Clínica Universidad de Navarra and CIBERONC, Pamplona 31008, Spain. [4]Medical Oncology Department, Hospital 12 de Octubre, Madrid 28041, Spain. [5]Medical Oncology Department, Institut Català d'Oncologia, Barcelona 08908, Spain. [6]Medical Oncology Department, Hospital Universitario Quirónsalud, Madrid 28223, Spain. [7]Medical Oncology Department, Clínica Universidad de Navarra, Pamplona 31008, Spain. [8]Radiology Department, Hospital General Universitario Gregorio Marañón, Madrid 28007, Spain. [9]Radiology Department, Hospital Ramón y Cajal, Madrid 28034, Spain. [10]Highlight Therapeutics (formerly known as Bioncotech Therapeutics), Valencia 46980, Spain.
*Corresponding author. Email: ivanpantic@hotmail.com
†These authors contributed equally to this work.

Early studies in experimental melanoma models with intravenous administration of a previous format of poly I:C–PEI demonstrated tumor cell death driven by accelerated autophagy, and helicase MDA5 and NOXA activation *(15)*. Preclinical experiments in mice with BO-112 administered intratumorally demonstrated that intralesional BO-112 exerts an antitumor activity accompanied by an increase in $CD8^+$ tumor-infiltrating lymphocytes and systemic cytotoxic T lymphocyte (CTL)–mediated immune responses. This therapeutic response is IFN-γ and IFN-α/β dependent and is observed not only in locally injected tumors but also in distant ones; the systemic effect is enhanced by the coadministration of anti–PD–ligand 1 (PD-L1) antibodies (*16*). In addition, intratumoral BO-112 is able to revert the resistance of Janus kinase 1 (*Jak1*)–deficient murine tumors to adoptive T cell therapy by restoring major histocompatibility complex (MHC) class I expression, thereby demonstrating the activity of BO-112 independent of tumor-intrinsic IFN signaling (*17*).

Here, we communicate the safety, the antitumor activity, and the accompanying immunobiological results of the first-in-human clinical trial of intratumoral BO-112 (NCT02828098). We focus on its activity in combination with anti–PD-1 monoclonal antibodies (mAbs) nivolumab or pembrolizumab in patients with solid tumors showing primary refractoriness to anti–PD-1 checkpoint blockade.

RESULTS

Clinical trial description and patient characteristics

This was a phase 1 clinical trial with four cohorts. The first three cohorts explored the safety and immunobiological effects of intratumoral BO-112 as a monotherapy using different doses (0.6 and 1 mg) and total numbers of injections (one to three) in solid malignant tumors. These three cohorts of a total of 16 patients led us to establish 1 mg as the recommended dose to test in combination with systemically administered anti–PD-1 mAbs in a fourth cohort. Cohort 4 included 28 patients who had previously started treatment with anti–PD-1 mAbs, either pembrolizumab or nivolumab, and had progressive disease (PD) as best response. These patients were then treated with an induction phase of intratumoral BO-112 followed by the combination of BO-112 with the anti–PD-1 agent that the patient had previously received, until PD as assessed by RECIST 1.1, intolerable toxicity, or death. Figure 1 summarizes the clinical trial flow (see data file S1 for the full protocol) and the patient grouping, in addition to a treatment schedule schema. Table 1 summarizes the main patient characteristics from cohorts 1 to 3, and Table 2 summarizes the main relevant patient characteristics (including previous treatments) from cohort 4.

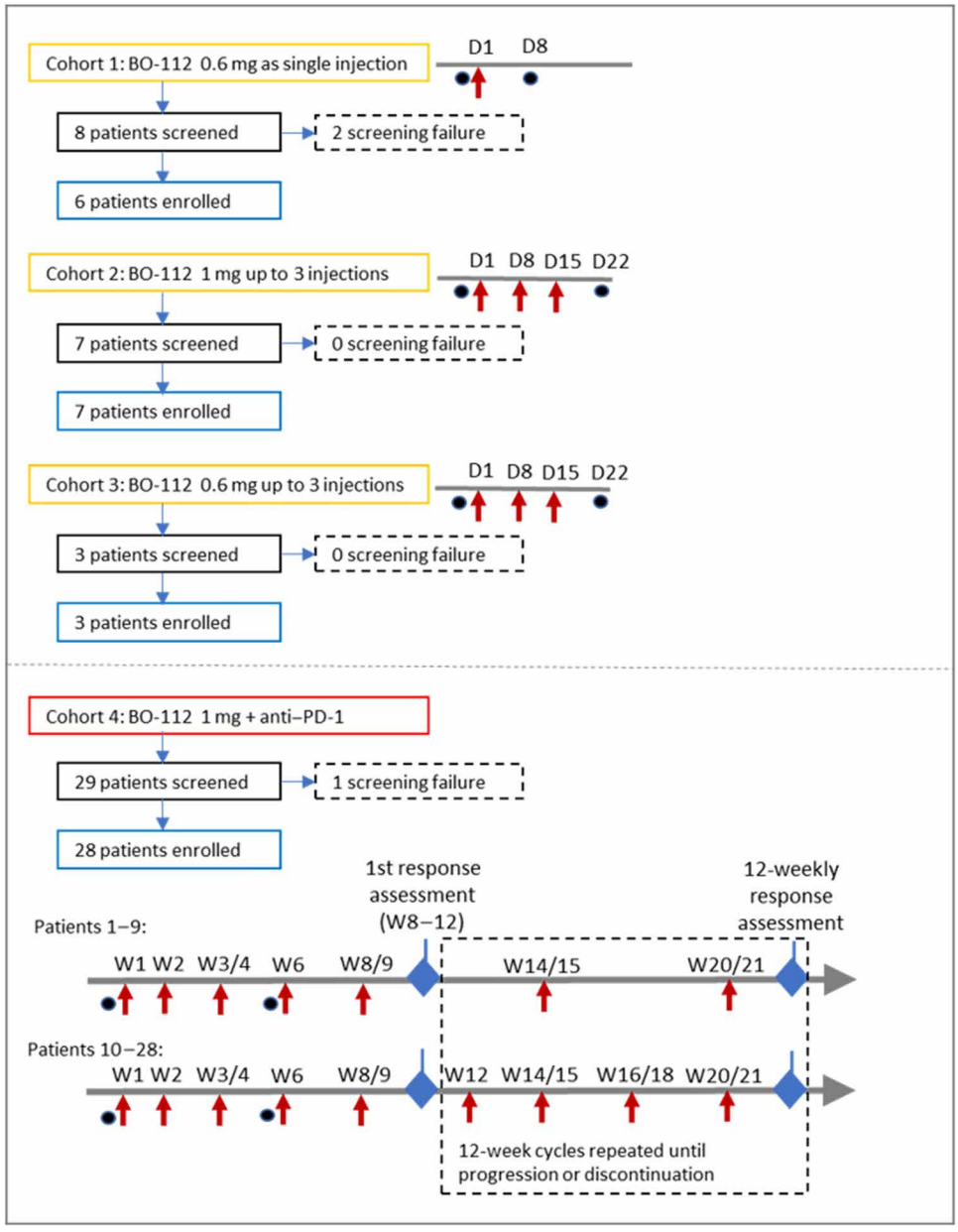

Fig. 1. CONSORT diagram of patient screening and enrollment for each of the four treatment cohorts. Intratumoral BO-112 injections are indicated by red arrows. Patients treated in cohort 4 with nivolumab were treated with one dose of BO-112 before reintroducing nivolumab every 2 weeks, whereas patients on pembrolizumab were treated with two doses of BO-112 before reintroducing pembrolizumab every 3 weeks until progression or discontinuation. BO-112 injections were administered on the same day and before the anti–PD-1 intravenous infusion. Solid black circles represent tumor biopsies: "pre-treatment" biopsy was on day 1 in week 1 before BO-112 for cohorts 1 to 4; "post-treatment" was 7 days after the last BO-112 injection in cohorts 1 to 3 and on day 36 in week 6 before the BO-112 injection in cohort 4.

Table 1. Demographic, pathological, and clinical characteristics of patients treated in cohorts 1 to 3.

Characteristics	Part 1			
	Cohort 1 *n* = 6	Cohort 2 *n* = 7	Cohort 3 *n* = 3	Total *n* = 16
Median age, years (range)	61 (49–73)	58 (42–74)	58 (46–78)	58 (42–78)
Male (%), female (%)	2 (33), 4 (67)	2 (29), 5 (71)	1 (33), 2 (67)	5 (31), 11 (69)
Tumor type, *n* (%)				
Melanoma	4	1	0	5 (31)
Leiomyosarcoma	0	2	1	3 (19)
Breast carcinoma	1	1	0	2 (13)
Other (adenoid cystic carcinoma, colorectal cancer, endometrial neuroendocrine carcinoma, head and neck cancer, ovarian cancer, and mesothelioma; *n* = 1 per type)	1	3	2	6 (38)
Previous lines of oncology therapy, *n* (%)				
0	0	0	0	0
1	1	1	0	2 (13)
2 or more	5	6	3	14 (88)
Previous radiotherapy, *n* (%)	4	6	1	11 (69)
Site of target (injected) lesion, *n* (%)				
Skin/subcutaneous nodule	2	4	0	6 (38)
Lymph node	2	2	0	4 (25)
Soft tissue	2	0	2	4 (25)
Liver	0	1	1	2 (13)

Safety of BO-112 alone and in combination with anti–PD-1 agents

Table 3 summarizes the safety findings according to Common Terminology Criteria for Adverse Events (CTCAE) v4.0 in the monotherapy cohorts and in the combination cohort. In general, BO-112 was well tolerated, with mild local and systemic reactions, including low-grade fever, possibly due to activation of type I IFNs. Thrombocytopenia (n = 2, single agent) and immune-related pneumonitis (n = 1, combination treatment) were the only BO-112–related grade 3 or 4 adverse events. There were no treatment-emergent adverse events (TEAEs) considered at least possibly related to BO-112 that occurred in four (25%) or more patients.

In cohort 4, the combination of BO-112 plus the corresponding anti–PD-1 agent did not lead to unexpected or more severe toxicities than the ones expected with these treatments, nor was there any observable exacerbation of BO-112–related adverse events. No deaths were attributed to BO-112 as monotherapy or in combination. BO-112 was not detected systemically in any of the 44 patients included in the four cohorts of the clinical trial.

BO-112 and anti–PD-1 tumor response according to RECIST 1.1

Among the 28 patients treated with the combination in cohort 4, 9 patients discontinued the treatment before the first scheduled response assessment, due to either a TEAE (n = 2) or evidence of disease progression (n = 7), and did not receive the protocol-specified five administrations of BO-112 (6 patients received only one or two administrations, 1 received three administrations, and 2 received four administrations). Nineteen patients received the protocol-prescribed five administrations of BO-112 before the first scheduled response assessment in weeks 8 to 12, and of these, 13 patients continued with further treatment. Among these 13 patients with metastatic lesions at multiple sites, 3 experienced a partial response (PR) and 10 had stable disease (SD) as the best overall responses by RECIST 1.1 criteria (Fig. 2). The three patients who achieved a response were a female patient, 48 years old, diagnosed with a wild-type BRAF cutaneous melanoma refractory to nivolumab; a male patient, 29 years old, with maxillary mucosal melanoma, wild-type BRAF, refractory to a combination of ipilimumab and nivolumab; and a male patient, 45 years old, with renal carcinoma who had progressed on previous therapies with sunitinib, cabozantinib, everolimus, and nivolumab. The two patients with melanoma and PR completed the 1-year per protocol combination of BO-112 and nivolumab. After the data cutoff for the analysis presented here, one of these patients with cutaneous melanoma was evaluated by positron emission tomography (PET)–computed tomography (CT) scan. The investigation showed ongoing major metabolic response (+80 weeks).

Table 2. Demographic, pathological, and clinical characteristics, including previous anti–PD-1 exposure of patients treated in cohort 4. SCCHN, squamous cell carcinoma of the head and neck; RCC, renal cell carcinoma.

Cohort 4, *n* = 28	
Characteristics	***n* (%)**
Median age, years (range)	59.5 (29.0–74.0)
Male and female	16 (57.1) and 12 (42.9)
Tumor type	
Melanoma	10 (35.7)
NSCLC	13 (46.4)
SCCHN	4 (14.3)
RCC	1 (3.6)
Previous lines of oncology therapy	
0	6 (21.4)
1	10 (35.7)
2 or more	12 (42.9)
Site of injected lesion*	
Skin/subcutaneous nodule	6 (21.4)
Lymph node	12 (42.9)
Soft tissue—nonvisceral	7 (25.0)
Lung	4 (14.3)
Liver	1 (3.6)
Anti–PD-1 antibody	
Nivolumab†	20 (71.4)
Pembrolizumab‡	8 (28.6)

*Eight patients (five with melanoma and three with NSCLC) had additional lesion(s) injected for some subsequent BO-112 administrations. †Two patients started nivolumab as part of a combination therapy rather than as single agent (one with daratumumab and one with cisplatin, pemetrexed, and ipilimumab), one patient was switched from atezolizumab to nivolumab, and one patient had previously progressed on pembrolizumab. ‡One patient had previously progressed on nivolumab.

Furthermore, a biopsy of one of the injected lesions (skin lesion in the gluteal region), taken when injections of BO-112 were no longer feasible due to tumor shrinkage, revealed an absence of tumor cells. The patient with mucosal melanoma still maintains the objective PR (+60 weeks), whereas the patient with clear cell renal cancer experienced PD after 20 weeks of response. The differences between injected and noninjected lesions are presented in fig. S1.

To analyze whether the combination of BO-112 and anti–PD-1 agents could have been detrimental for some of the patients, we analyzed the pre- and post-study progression-free survival (PFS) periods in patients with PD as best response. PFS before and after study treatment was analyzed for patients whose best response was PD. As shown in table S1, no apparent hyperprogressive patterns have been noticed.

Antitumor and immunobiological effects of BO-112 in combination with anti–PD-1 agents

Studying patients with evaluable pre- and post-treatment formalin-fixed and paraffin-embedded (FFPE) samples in cohorts 1 to 3 (n = 13), we observed at least 5% increase in apoptosis in 77% of the patients and at least 5% increase in necrosis in 46% of the patients in post–BO-112 treatment biopsies. In cohort 4 (with evaluable paired biopsies, n = 19), these increases were observed in 11 and 53% of the patients for apoptosis and necrosis, respectively (table S2).

In cohorts 1 to 3, at least 5% increases in T cell infiltration were observed in 36% of the patients for CD4 and in 23% of them for CD8 (n = 11 for CD4 and n = 13 for CD8). More than 5% increases in T cell infiltration were also observed in cohort 4: 21% for CD4 and 37% for CD8 in evaluable paired biopsies (n = 19) (table S2).

Representative multiplex staining showing CD8 increase in three patients is in fig. S2. PD-L1 expression was increased by at least 5% in 17% of the patients in cohorts 1 to 3 (evaluable, n = 12), in contrast with 0% of the patients in cohort 4 (evaluable, n = 19) (table S2).

In the histology specimens, we observed statistically significant increases in apoptosis (P = 0.002) and CD4 T cell counts (P = 0.0352) in cohorts 1 to 3 and necrosis in cohort 4 (P = 0.0054) (fig. S3). Moreover, we observed a statistically significant increase of $CD8^+$ (P = 0.0335), but not $CD4^+$ T cells, after intratumoral injection of BO-112 in combination with an anti–PD-1 agent in patients from cohort 4 who achieved PR or SD when compared to those who had PD (fig. S3).

Figure 3A shows the density of immune cells in tumor biopsies before and after BO-112 treatment in cohort 4 (combination treatment). Statistically significant increases in $CD8^+$ T cell immunostaining (P = 0.0078) and necrosis (P = 0.0054; fig. S3) were detected in the two patients with melanoma who achieved PR and in one patient with BRAF mutant melanoma who had been resistant to several previous lines of targeted therapy and immune therapies but achieved SD in our trial, whose measurable tumor burden decreased 32% by RECIST 1.1 (Fig. 3B).

Thirteen paired pre- and post-treatment flash-frozen samples from cohorts 1 to 3 were available for immune gene expression analysis using the nCounter PanCancer Immune Profiling Panel (NanoString Technologies Inc.). In some patients, BO-112 treatment resulted in the up-regulation of gene clusters (fig. S4) associated with an efficient antitumor immune response described by Ayers *et al.* (*18*). The evaluation of gene expression changes between pre- and post-treatment biopsies from all patients did not find statistically significant differences (table S3).

In cohort 4, 19 of the 28 patients had paired pre- and post-treatment flash-frozen biopsies. The objective was to analyze the immune gene expression patterns using the same NanoString technology panel. We found a low degree of variability in expression in tumors among patients and thus were unable to define an expression pattern that could differentiate the responders from those who experienced progression upon treatment (fig. S5). The same negative result was also obtained when the analysis included only the normalized pre-treatment expression data. Nonetheless, on the basis of the analysis of the post-treatment expression profiles of all genes from the NanoString panel, we obtained a specific BO-112 gene signature that best defined the outcome of treatment (Fig. 4A). The conditions for the unsupervised clustering were based on the clinical outcome, and only normalized expression data obtained from post-treatment biopsies (taken from injected lesions) were used. When we used post-treatment expression data alone, we obtained a consistent gene set that allowed clustering

Table 3. Description of the most relevant TEAEs. The table includes TEAEs that were observed in three (19%) or more patients from BO-112 monotherapy cohorts 1 to 3 and in three (10%) or more patients from cohort 4, BO-112 combined with anti–PD-1.

Adverse event (preferred term)	All TEAEs *n* (%)				TEAEs related to BO-112 *n* (%)			
	All		Grades 3–5		All		Grades 3–5	
	Cohorts 1–3	Cohort 4	Cohorts 1–3	Cohort 4	Cohorts 1–3	Cohort 4	Cohorts 1–3	Cohort 4
	n = 16	*n* = 28	*n* = 16	*n* = 28	*n* = 16	*n* = 28	*n* = 16	*n* = 28
Anemia	2 (12.5)	5 (17.9)	1 (6.3)	1 (3.6)	0	0	0	0
Abdominal pain	1 (6.3)	7 (25.0)	1 (6.3)	1 (3.6)	0	0	0	0
Constipation	2 (12.5)	6 (21.4)	1 (6.3)	0	0	0	0	0
Diarrhea	0	8 (28.6)	0	1 (3.6)	0	0	0	0
Dry mouth	2 (12.5)	4 (14.3)	0	0	0	2 (16.7)	0	0
Nausea	4 (25.0)	13 (46.4)	0	0	1 (6.3)	7 (25.0)	0	0
Vomiting	2 (12.5)	7 (25.0)	0	0	1 (6.3)	4 (14.3)	0	0
Asthenia	4 (25.0)	16 (57.1)	1 (6.3)	0	0	9 (32.1)	0	0
Chills	2 (12.5)	7 (25.0)	0	0	2 (12.5)	6 (21.4)	0	0
Fatigue	3 (18.8)	3 (10.7)	0	0		2 (7.1)		0
Injection site pain	1 (6.3)	5 (17.9)	0	0	1 (6.3)	3 (10.7)	0	0
Pain	2 (12.5)	6 (21.4)	0	1 (3.6)	0	0	0	0
Pyrexia	4 (25.0)	21 (75.0)	0	0	3 (18.8)	18 (64.3)	0	0
Respiratory tract infection	2 (12.5)	4 (14.3)	0	2 (7.1)	0	0	0	0
Decreased appetite	1 (6.3)	9 (32.1)	0	0	0	4 (14.3)	0	0
Back pain	2 (12.5)	5 (17.9)	1 (6.3)	1 (3.6)	0	0	0	0
Musculoskeletal pain	0	4 (14.3)	0	1 (3.6)	0	1 (3.6)	0	0
Myalgia	2 (12.5)	7(25.0)	0	0	1 (6.3)	6 (21.4)	0	0
Neck pain	0	3 (10.7)	0	0	0	0	0	0
Tumor pain	0	3 (10.7)	0	1 (3.6)	0	0	0	0
Dizziness	1 (6.3)	5 (17.9)	0	0	0	2 (7.1)	0	0
Dysgeusia	0	4 (14.3)	0	0	0	2 (7.1)	0	0
Headache	3 (18.8)	6 (21.4)	0	0	2 (12.5)	1 (3.6)	0	0
Syncope	0	4 (14.3)	0	2 (7.1)	0	0	0	0
Anxiety	0	5 (17.9)	0	0	0	0	0	0
Insomnia	1 (6.3)	4 (14.3)	0	0	0	0	0	0
Cough	0	4 (14.3)	0	0	0	0	0	0
Dyspnea	0	5 (17.9)	0	0	0	0	0	0
Productive cough	0	6 (21.4)	0	0	0	0	0	0
Respiratory disorder	0	4 (14.3)	0	0	0	0	0	0
Pruritus	0	6 (21.4)	0	0	0	3 (10.7)	0	0

of patient groups depending on the clinical benefit. As shown in the heatmap (Fig. 4A), genes associated with T cell cytotoxic activity (for instance, *GZMB* and *KLRK1*) were induced in patients who experienced PR or SD. Furthermore, several genes appeared to be down-regulated in patients benefiting from treatment (*IL13RA2*, *MAGEeC2*, *CTCFL*, and *SERPINB2*).

The volcano plot in Fig. 4B shows the global post-treatment gene expression changes between the evaluated patient categories, namely, benefit (PR + SD) versus no benefit (PD). Significantly up- or down-regulated genes are highlighted as red dots (P cutoff = 0.01). The gene expression analysis and statistical parameters are summarized in table S4. Raw data of all gene analyses performed are available in

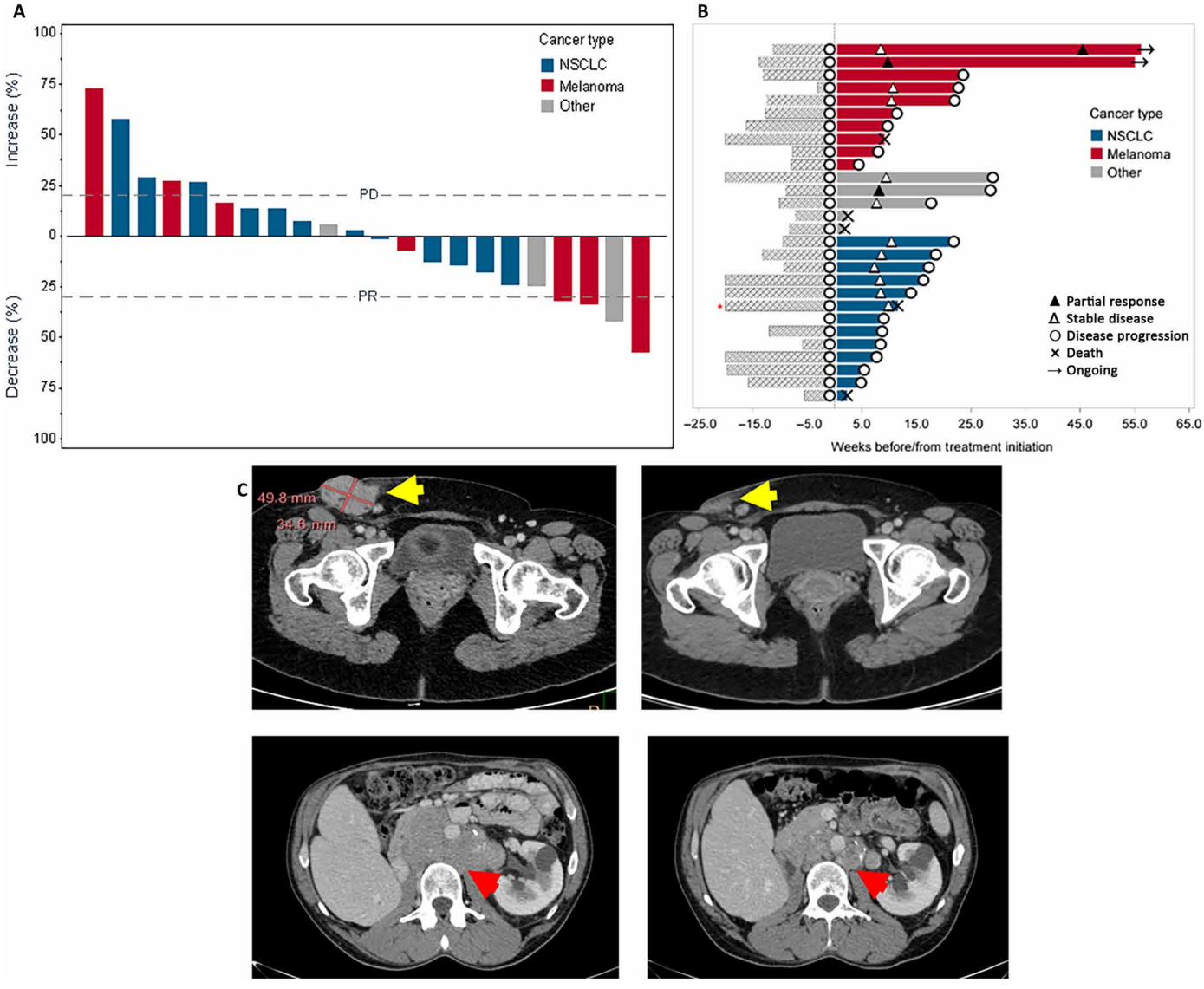

Fig. 2. Response assessments of patients treated in the combination cohort. (**A**) Waterfall plot for RECIST 1.1 best objective response. Waterfall plot is missing nine patients, because eight patients either died or had disease progression before the first scheduled response assessment, and one patient was not evaluable due to irradiation of his RECIST target lesion. (**B**) Modified swimmer plot for PFS. The shaded gray bars on the left side of the swimmer plot represent the anti–PD-1 agent exposure time (weeks) before study entry. Red asterisk corresponds to a patient that had a prestudy period >30 weeks. Swimmer plot is based on intention to treat and has all the patients. (**C**) CT scans of two of the three patients with objective response (basal scans on the left, first on-treatment evaluation scans at 9 or 10 weeks on the right). Top: Female patient with BRAF wild-type melanoma refractory to nivolumab. Bottom: Male patient with renal carcinoma refractory to sunitinib, cabozantinib, everolimus, and nivolumab. Yellow arrows indicate BO-112–injected lesions, and red arrows indicate noninjected lesions.

data file S2. As expected, when the analyzed gene signatures were ranked according to their enrichment score, those associated with T cell cytotoxic activity and the defined BO-112 signature were located at the top of the ranking (Fig. 4C).

DISCUSSION

Patients with tumors refractory to anti–PD–(L)1 constitute a paramount priority in clinical oncology. Currently, no randomized trial results are available for this refractory population in any of the approved tumor indications of these drugs, in either the second- or first-line treatment setting. Thus, it is highly recommended to include these patients in combination clinical trials. The knowledge of the tumor-intrinsic mechanisms of resistance to immunotherapy is exponentially growing (*19*), thus expanding the current landscape of clinical trials; intratumoral therapeutic approaches are among these strategies.

Here, we report an approach in the anti–PD-1-refractory setting using BO-112, a synthetic nanoplexed dsRNA (poly I:C). As monotherapy, BO-112 demonstrated a good safety profile, which was also observed in combination with anti–PD-1 mAb. Three patients with tumors refractory to anti–PD-1 had objective responses, which

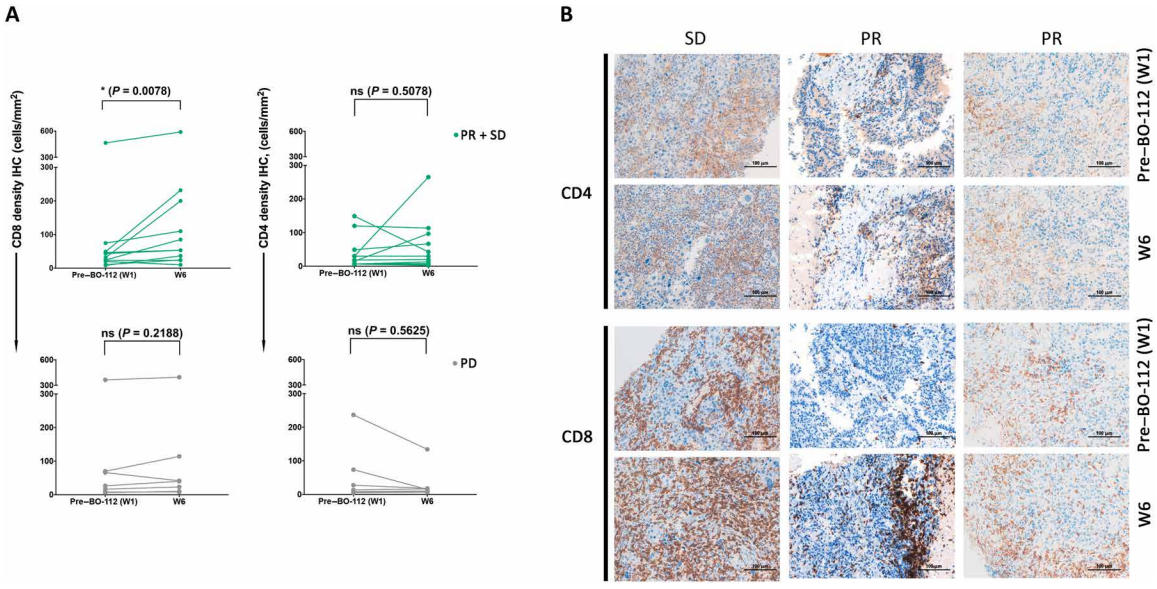

Fig. 3. Evaluation of immune cells in biopsies before and after BO-112 treatment. (**A**) Pre- and post-treatment intratumoral $CD8^+$ and $CD4^+$ T cell density in patients treated with the combination of BO-112 and anti–PD-1 agents in cohort 4. ns, not significant. (**B**) Representative IHC images showing $CD8^+$ and $CD4^+$ T cell infiltrates in two patients with PR and one patient with SD. Scale bars, 100 μm.

included noninjected, distant lesions. Corresponding changes in intratumoral immune activation were observed in response to BO-112 by immunohistochemistry (IHC) and gene expression analysis.

In melanoma, the most clinically advanced intratumoral therapy is T-VEC, a genetically modified herpes simplex type I virus that has been approved as a monotherapy in some countries (*20*). Its activity in combination with the anti–PD-1 agent pembrolizumab (in anti–PD-1–naïve melanoma patients) has been published in a phase 1 clinical trial that showed a 62% response rate (*3*). However, no experience in patients with PD-1–refractory tumors has yet been reported. Responders to the combination had an increase in $CD8^+$ T cell infiltration and IFN-γ gene signature (*3*), similar to what we have observed in response to BO-112 and anti–PD-1. These promising overall response rate data for the combination of intratumoral immune virotherapy and pembrolizumab are being tested in a randomized clinical trial of T-VEC plus pembrolizumab versus intratumoral placebo plus pembrolizumab, whose results are pending (NCT02263508).

In the anti–PD-1–refractory setting, several intratumoral immunotherapy compounds have been used. The TLR9 agonist SD-101 in combination with pembrolizumab in melanoma patients resulted in an overall response rate of 15% in patients with anti–PD-1–refractory tumors (*21*). In cohort 4 of our study, 2 of 10 patients with melanoma achieved a PR in this refractory setting. The results of SD-101 combined with pembrolizumab were far better in the anti–PD-1–naïve patients, in whom a 78% overall response rate was observed (*21*).

We are aware of only one trial in non–small cell lung cancer (NSCLC) combining the intratumoral administration of the TLR9 agonist CMP-001 with an anti–PD–(L)1 agent and radiotherapy after failure of previous anti–PD–(L)1 treatment (NCT03438318), likely because intratumoral treatment approaches have focused on skin cancers where there are often accessible lesions for direct intratumoral injection. Our study included 13 patients with NSCLC in cohort 4, who were treated with BO-112 and anti–PD-1 mAb and achieved SD at the first radiological evaluation in 6 of these patients.

Recently, poly ICLC (Hiltonol) has been administered intratumorally to a series of non-Hodgkin's lymphoma patients with good safety, efficacy, and immunological effects in combination with low-dose radiotherapy and sFLT3L (*9*). A combination of local delivery of BO-112 with radiotherapy may warrant evaluation for solid tumors.

Intratumoral BO-112 has demonstrated an acceptable safety profile, similar to that described with other intratumoral immunotherapy treatments such as T-VEC (*3*) and SD-101 (*21*). Unlike T-VEC or other oncolytic viruses, BO-112 administration does not require additional safety measures related to the biosafety of a viral-based therapy. The grade 3 to 4 thrombocytopenia adverse events experienced by two of the patients in our study were rapidly resolved in both cases and have not occurred in the combination cohort.

The evaluation of pre- and on-treatment core needle biopsies of treated tumors suggests the instigation of a potent IFN response in response to treatment. This is consistent with the mechanism of action of BO-112, which engages pattern recognition receptors (for example, TLR3 and MDA5, among others), resulting in downstream activation of type I IFN signaling. Treatment also resulted in tumor infiltration by $CD8^+$ T cells, especially in patients with PR or even SD. Although the correlation of response or clinical benefit with gene expression profiling or IHC is preliminary due to the small number of patients, increased IFN gene expression and T cell infiltration are consistent with tumor microenvironment changes seen in patients responding to immune checkpoint blockade (*22*, *23*). In addition, we postulate a mechanistic connection between innate and adaptive immune systems, as previously proposed by investigators associated with our group (*16*) in mouse preclinical models. This is supported by the increase in genes related to type I and II IFN responses upon BO-112 treatments in monotherapy or in combination. Such changes were also observed in preclinical studies. No changes in circulating cytokines or lymphocyte subsets were found in peripheral blood.

Our study is limited by the small number of patients included and the mixed population, which is in the nature of a first-in-human phase 1 clinical trial designed for safety, dose finding, and exploration

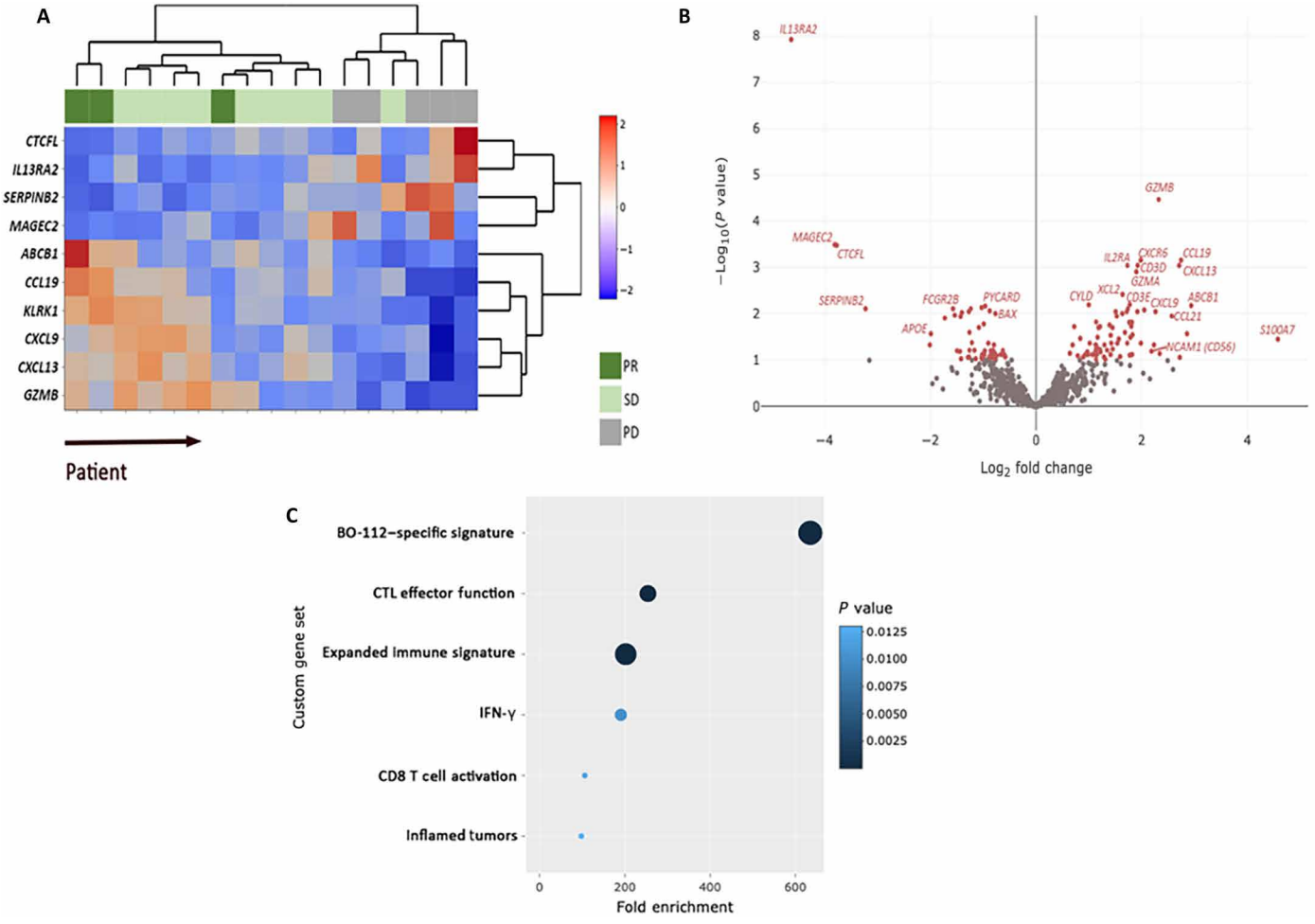

Fig. 4. Gene expression profiles upon BO-112 treatment. (**A**) Specific BO-112 gene expression signature obtained for the BO-112 plus anti–PD-1 combination cohort 4 ($n = 17$). The post-treatment expression profiles of these 10 genes allowed us to classify the patients according to their overall response assessment (RECIST 1.1), annotated in the top row (dark green, PR; light green, SD; gray, PD). (**B**) Volcano plot representing the changes in post-treatment gene expression when comparing tumor samples from patients who had PR or SD as best response with samples from patients whose best response was PD (no benefit) after treatment with intratumoral BO-112 and an approved anti–PD-1 antibody systemically (statistically significantly up- and down-regulated genes are depicted in red, $-\log_{10}$ [*P* value]). (**C**) Enrichment analysis of the specified gene signatures. The color scale associated with the heatmaps refers to the relative gene expression as compared to baseline ($\log_2$ [ratio]).

of potential immunobiological markers of antitumoral activity and clinical benefit. These could be the main reasons for not detecting an increase in pre- and post-treatment ratios of known gene expression signatures. The description of a putative BO-112 signature selecting the genes that may distinguish patients with or without clinical benefit could help define a predictive gene signature to be validated in ensuing clinical trials.

One of the genes observed to be down-regulated in patients benefiting from BO-112 is interleukin-13 receptor α2 (*IL13Rα2*). This has been recently described as a factor acting as a functional cancer gene when overexpressed in cases of melanoma (*24*). This preliminary signature should be validated in larger studies to analyze its real predictive or prognostic values.

Another limitation is that patients in cohort 4 must have had PD as best response while on anti–PD-1 (or SD within 6 months followed by PD) as per protocol, defined with radiological progression at the time of study entry. To avoid further treatment delays, PD was not required to be confirmed by subsequent CT scan. This could raise the question of whether the PRs observed in our study were resulting from the combination or were delayed responses. Although the phenomenon of tumor pseudo-progression followed by delayed response has been observed early in the development of immunotherapy (*25*), in larger pooled studies this event is described in as few as 4% of the immunotherapy-treated patients (specifically in patients with melanoma), and thus, the U.S. Food and Drug Administration (FDA) does not recommend to treat beyond progression (*26*). In our case, the two responding patients with melanoma would represent a 20% response rate (2 of 10) and both showed increased $CD8^+$ T cell infiltration after the first three administrations of BO-112 compared to the status at the time of anti–PD-1 progression (study baseline). However, the number of patients is too low to draw a formal conclusion about the responses because the main objective of this first-in-human clinical trial was safety. Larger studies will be needed to confirm the clinical activity of the combination.

Tumor hyperprogression is a newly raised concern in the immunotherapy research community, and it can be difficult to distinguish

between natural evolution of the disease and an impairment due to the treatment (*27*). This is particularly concerning when evaluating new drugs and combinations. In our study, considering the above-mentioned limitations, we did not detect signals of faster progression in patients whose best response was PD.

In conclusion, this early clinical trial demonstrates that a combination of intratumoral BO-112 and anti–PD-1 agents had a manageable toxicity profile and produced evidence of clinical activity in the anti–PD-1–refractory setting. Furthermore, intratumoral BO-112 demonstrated signs of immunobiological activity in the tumor microenvironment, mainly through an increase in signs of local IFN activity and infiltration by active $CD8^+$ T cells. Overall, intratumoral BO-112 could be a potential therapeutic tool to overcome primary resistance to anti–PD-1 therapy. Safety, clinical activity, and pharmacodynamic observations warrant further investigation and clinical development of the strategy.

MATERIALS AND METHODS

Study design

The study protocol is available in its current version as data file S1. This was a phase 1 exploratory, open-label study in adult patients (defined as ≥18 years old) with advanced or metastatic cancer with biopsy-accessible tumors. The study consisted of two parts. Part 1 evaluated the biological effect and safety/tolerability, pharmacodynamics, and pharmacokinetics of the intratumoral administration of BO-112 as a single agent in a standard 3 + 3, escalating dose study design, both as single-dose and multiple-dose administrations (1-week intervals, three doses). Patients with any solid tumor type, for whom no standard of care treatments were available and who had at least one biopsy-accessible lesion, were eligible for part 1. The primary end point in part 1 was biological effect, with safety and tolerability, pharmacokinetics, and pharmacodynamics as secondary end points.

An expansion cohort (part 2) was added and consisted of patients who were treated with nivolumab or pembrolizumab for a cancer indication approved in Europe and were primarily resistant to anti–PD-1 therapy, defined as patients who had PD as best response or had SD that lasted less than 6 months. Patients had to have radiological disease progression, as well as at least one biopsy-accessible lesion to be eligible. These patients received either one or two single-agent BO-112 intratumoral administrations at 1-week intervals, followed by the combination of BO-112 with intravenous infusion of nivolumab as of week 2 or pembrolizumab as of week 3 at the approved dose and schedule (Fig. 1). Treatment continued until disease progression, unacceptable toxicity, or patient withdrawal. The primary end point was safety and tolerability of the combination, with antitumoral and biological activity, pharmacodynamics, and pharmacokinetics as secondary end points.

Compliance with ethical standards

All patients signed an informed consent before entering the clinical trial. Central Ethics Committee approval was obtained by Clínica Universidad de Navarra.

BO-112 administration

BO-112 was administered in a previously selected tumoral lesion sized 1 cm or more that was amenable to intratumoral injection. Ultrasound guidance by a radiologist was generally performed. The chosen lesion for injection was the same lesion injected throughout the clinical trial, unless it became too small to be injected. In that case, if another lesion(s) was (were) available, then BO-112 was divided between the remaining lesion and a new one, or new ones if the first lesion disappeared. The total volume (BO-112 diluted in 5% glucose) for 0.6 mg was 1 ml, and for 1 mg, it was 2 ml.

Pathological specimen preparation

Pre- and post-treatment biopsies (lesions chosen for injection were biopsied before and after BO-112) were prepared for IHC. Fine-needle core biopsies were collected from tumor lesions before and after the injection of BO-112, for each patient, following the protocol procedure schedule. Pretreatment biopsies were performed the day before or the day of (but before) the first injection of BO-112. Post-treatment biopsies were planned at 8 days after any injection in part 1 and after three BO-112 injections in part 2, namely, on day 36, before the scheduled BO-112 injection in week 6 (Fig. 1). They were FFPE for hematoxylin and eosin (H&E) and IHC stains. Slides with 3-μm-thin cuts from FFPE samples were prepared for immunodetection with the following antibodies from Agilent-Dako: anti-CD4 (clone 4B12), anti-CD8 (clone C8/144B), and anti–PD-L1 (clone 22C3). Data were analyzed descriptively, and this analysis included the percentage of positive cells for each marker analyzed (CD4, CD8, and PD-L1) in two to four microscopic fields and the percentage of necrosis in the tumor lesion (referred to as tumor area). All techniques and evaluations were performed at the Laboratory of Pathology in MD Anderson-Madrid (Spain).

NanoString analysis of the expression of specific gene signatures was performed after a supplementary informed consent for genetic testing was signed by enrolled patients. NanoString nCounter Technology was used for the expression assessment. We used the nCounter PanCancer Immune Profiling Panel, which contains genes covering both the adaptive and innate immune responses. Total RNA from two tumor biopsies was analyzed for the same patients before and after injection of BO-112, as stated in the protocol and mentioned above. The tumor biopsies were immediately rinsed in RNAlater (Thermo Fisher Scientific) after their collection to preserve the nucleic acids' integrity. The total RNA was isolated by TRIzol (Thermo Fisher Scientific), following the manufacturer's instructions, and the integrity/quality was assessed by Bioanalyzer technology (Agilent). The tests were performed at the Laboratory of Translational Oncology (Hospital General Universitario Gregorio Marañón, Madrid, Spain), and the bioinformatic analyses were performed at DREAMgenics (Oviedo, Spain) following the manufacturer's instructions (NanoString). Gene expression raw data are available in data file S2.

BO-112 pharmacokinetics

Whole blood (3 ml) was drawn at specific time points by venous puncture or permanent venous catheter into EDTA-containing polypropylene tubes. The samples were placed immediately in ice and subsequently (within 30 min after collection) centrifuged at 1700*g* at a temperature between 3° and 5°C for 10 min to obtain the plasma. The samples were frozen immediately and stored at −80°C (±10°C). Pharmacokinetic evaluations of BO-112 were performed at the bioanalytical laboratory (Accelero Bioanalytics GmbH, Berlin, Germany) by a ligand-binding assay technique [enzyme-linked immunosorbent assay (ELISA)] using two specific antibodies against the active ingredient of BO-112 (poly I:C) previously extracted from plasma. Plasma concentrations were determined using a lower limit of quantification of 62.5 ng/ml.

Response evaluation for cohort 4

A baseline CT scan was obtained in the 28 days before the first BO-112 administration. The first study CT scan was scheduled in weeks 8 to 12. Subsequent CT scans were obtained every 10 to 14 weeks to evaluate the responses by RECIST 1.1 criteria.

Statistical analysis

Clinical data, including efficacy and safety evaluations, were descriptive, using percentages when needed, and no formal comparisons could be done. As described above, data from histological studies were analyzed descriptively (in Fig. 3A, $CD8^+$ and $CD4^+$ cell densities were assigned by recording the cell number in two to four fields of 1 mm^2 each/sample and shown for each patient). Wilcoxon matched-pairs signed-rank test was used to compare pre- and post-treatment biopsies for paired samples and *U* Mann-Whitney test for unpaired samples; *P* values of <0.05 were considered statistically significant. For the NanoString studies, counts from cohorts 1 to 4 were extracted using nCounter Software (NanoString Inc.), but the normalization was different between data from cohorts 1 to 3 and cohort 4.

Using the nSolver Analysis Software (NanoString Inc.), counts from cohorts 1 to 3 were first normalized to the geometric mean of the negative control spiked into the assay to correct for experimental variability. Then, the geometric mean was used to compute a normalization factor of positive control and, finally, normalized to housekeeping genes built into the Human Immunology panel. The normalized data were measured as counts. Normalized data of nSolver procedure were log-transformed (with base 2). The differential expression was evaluated using a paired *t* test for each gene. Paired *t* test was constructed using a linear model (the limma R package).

Absolute values of ratio $\log_2$ fold change for genes were obtained for each patient. Genes with ratios greater than 2 were considered up-regulated (post-treatment value greater than pre-treatment), and those with ratios smaller than −2 were considered down-regulated (post-treatment value less than pre-treatment).

For representation purposes, two immune gene signatures related to the potential therapeutic response and antitumor immunity of anti–PD-1 therapies [described in (*18*)] were evaluated before and after BO-112 treatment.

Counts from cohort 4 were normalized using RUVSeq R package (DOI: 10.1038/nbt.2931). Differential expression analysis was performed with DESeq2 algorithm (DOI: 10.1186/s13059-014-0550-8), with an adjusted *P* cutoff of 0.05; in addition, a $\log_2$ (fold change) of $\geq$2 and $\leq$−2 and an adjusted *P* cutoff of 0.01 were used to define a gene expression signature from post-treatment expression data: a set of genes that significantly differentiates the overall response conditions. Normalized gene expression heatmaps of particular gene sets were also represented (post-treatment data). Specific immune gene sets were classified according to their enrichment scores. This specific analysis was performed using pathfindR (DOI: 10.3389/fgene.2019.00858), with the adjusted *P* cutoff of 0.01 for differentially expressed genes.

SUPPLEMENTARY MATERIALS

stm.sciencemag.org/cgi/content/full/12/565/eabb0391/DC1
Fig. S1. Injected versus noninjected lesions.
Fig. S2. Multiplex immunofluorescence staining.
Fig. S3. Changes in apoptosis, necrosis, PD-L1, and CD8 and CD4 immunostaining after BO-112.
Fig. S4. Heatmaps of gene expression in cohorts 1 to 3.
Fig. S5. Unsupervised clustering of expression data in cohort 4.
Table S1. PFS pre- and post-study in patients experiencing PD.
Table S2. IHC findings.
Table S3. Adjusted gene expression analysis for cohorts 1 to 3.
Table S4. Gene expression analysis for BO-112 signature.
Data file S1. Study protocol version 7.0.
Data file S2. Gene expression raw data.

View/request a protocol for this paper from *Bio-protocol*.

REFERENCES AND NOTES

1. M. A. Aznar, N. Tinari, A. J. Rullán, A. R. Sánchez-Paulete, M. E. Rodriguez-Ruiz, I. Melero, Intratumoral delivery of immunotherapy—Act locally, think globally. *J. Immunol.* **198**, 31–39 (2017).
2. A. Marabelle, R. Andtbacka, K. Harrington, I. Melero, R. Leidner, T. de Baere, C. Robert, P. A. Ascierto, J.-F. Baurain, M. Imperiale, S. Rahimian, D. Tersago, E. Klumper, M. Hendriks, R. Kumar, M. Stern, K. Öhrling, C. Massacesi, I. Tchakov, A. Tse, J.-Y. Douillard, J. Tabernero, J. Haanen, J. Brody, Starting the fight in the tumor: Expert recommendations for the development of human intratumoral immunotherapy (HIT-IT). *Ann. Oncol.* **29**, 2163–2174 (2018).
3. A. Ribas, R. Dummer, I. Puzanov, A. VanderWalde, R. H. I. Andtbacka, O. Michielin, A. J. Olszanski, J. Malvehy, J. Cebon, E. Fernandez, J. M. Kirkwood, T. F. Gajewski, L. Chen, K. S. Gorski, A. A. Anderson, S. J. Diede, M. E. Lassman, J. Gansert, F. S. Hodi, G. V. Long, Oncolytic virotherapy promotes intratumoral T cell infiltration and improves anti-PD-1 immunotherapy. *Cell* **170**, 1109–1119.e10 (2017).
4. M. E. Rodríguez-Ruiz, J. L. Perez-Gracia, I. Rodríguez, C. Alfaro, C. Oñate, G. Pérez, I. Gil-Bazo, A. Benito, S. Inogés, A. López-Diaz de Cerio, M. Ponz-Sarvise, L. Resano, P. Berraondo, B. Barbés, S. Martin-Algarra, A. Gúrpide, M. F. Sanmamed, C. de Andrea, A. M. Salazar, I. Melero, Combined immunotherapy encompassing intratumoral poly-ICLC, dendritic-cell vaccination and radiotherapy in advanced cancer patients. *Ann. Oncol.* **29**, 1312–1319 (2018).
5. S. Bhatia, N. J. Miller, H. Lu, N. V. Vandeven, D. Ibrani, M. Shinohara, D. Byrd, U. Parvathaneni, R. M. Kulikauskas, J. Ter Meulen, F. J. Hsu, D. M. Koelle, P. Nghiem, Intratumoral G100, a TLR4 agonist, induces anti-tumor immune responses and tumor regression in patients with Merkel cell carcinoma. *Clin. Cancer Res.* **15**, 1185–1195 (2018).
6. A. R. Sánchez-Paulete, A. Teijeira, F. J. Cueto, S. Garasa, J. L. Pérez-Gracia, A. Sánchez-Arráez, D. Sancho, I. Melero, Antigen cross-presentation and T-cell cross-priming in cancer immunology and immunotherapy. *Ann. Oncol.* **28**, XII44–XII55 (2017).
7. N. Chen, P. Xia, S. Li, T. Zhang, T. T. Wang, J. Zhu, RNA sensors of the innate immune system and their detection of pathogens. *IUBMB Life* **69**, 297–304 (2017).
8. E. Gonzalez-Gugel, M. Saxena, N. Bhardwaj, Modulation of innate immunity in the tumor microenvironment. *Cancer Immunol. Immunother.* **65**, 1261–1268 (2016).
9. L. Hammerich, T. U. Marron, R. Upadhyay, J. Svensson-Arvelund, M. Dhainaut, S. Hussein, Y. Zhan, D. Ostrowski, M. Yellin, H. Marsh, A. M. Salazar, A. H. Rahman, B. D. Brown, M. Merad, J. D. Brody, Systemic clinical tumor regressions and potentiation of PD1 blockade with in situ vaccination. *Nat. Med.* **25**, 814–824 (2019).
10. H. R. Hubbell, K. Kvalnes-Krick, W. A. Carter, D. R. Strayer, Antiproliferative and immunomodulatory actions of beta-interferon and double-stranded RNA, individually and in combination, on human bladder tumor xenografts in nude mice. *Cancer Res.* **45**, 2481–2486 (1985).
11. W. M. Mitchell, D. C. Montefiori, W. E. Robinson Jr., D. R. Strayer, W. A. Carter, Mismatched double-stranded RNA (ampligen) reduces concentration of zidovudine (azidothymidine) required for in-vitro inhibition of human immunodeficiency virus. *Lancet* **1**, 890–892 (1987).
12. D. R. Strayer, W. A. Carter, I. Brodsky, P. Cheney, D. Peterson, P. Salvato, C. Thompson, M. Loveless, D. E. Shapiro, W. Elsasser, A controlled clinical trial with a specifically configured RNA drug, poly(I).poly(C12U), in chronic fatigue syndrome. *Clin. Infect. Dis.* **18** (suppl. 1), S88–S95 (1994).
13. K. A. O. Martins, S. Bavari, A. M. Salazar, Vaccine adjuvant uses of poly-IC and derivatives. *Expert Rev. Vaccines* **14**, 447–459 (2015).
14. M. Caskey, F. Lefebvre, A. Filali-Mouhim, M. J. Cameron, J.-P. Goulet, E. K. Haddad, G. Breton, C. Trumpfheller, S. Pollak, I. Shimeliovich, A. Duque-Alarcon, L. Pan, A. Nelkenbaum, A. M. Salazar, S. J. Schlesinger, R. M. Steinman, R. P. Sékaly, Synthetic double-stranded RNA induces innate immune responses similar to a live viral vaccine in humans. *J. Exp. Med.* **208**, 2357–2366 (2011).
15. D. Tormo, A. Checińska, D. Alonso-Curbelo, E. Pérez-Guijarro, E. Cañón, E. Riveiro-Falkenbach, T. G. Calvo, L. Larribere, D. Megías, F. Mulero, M. A. Piris, R. Dash, P. M. Barral, J. L. Rodríguez-Peralto, P. Ortiz-Romero, T. Tüting, P. B. Fisher, M. S. Soengas, Targeted activation of innate immunity for therapeutic induction of autophagy and apoptosis in melanoma cells. *Cancer Cell* **16**, 103–114 (2009).
16. M. A. Aznar, L. Planelles, M. Perez-Olivares, C. Molina, S. Garasa, I. Etxeberría, G. Perez, I. Rodriguez, E. Bolaños, P. Lopez-Casas, M. E. Rodriguez-Ruiz, J. L. Perez-Gracia, I. Marquez-Rodas, A. Teijeira, M. Quintero, I. Melero, Immunotherapeutic effects of intratumoral nanoplexed poly I:C. *J. Immunother. Cancer* **7**, 116 (2019).
17. A. Kalbasi, M. Tariveranmoshabad, K. Hakimi, S. Kremer, K. M. Campbell, J. M. Funes, A. Vega-Crespo, G. Parisi, A. Champekar, C. Nguyen, D. Torrejon, D. Shin, J. M. Zaretsky, R. D. Damoiseaux, D. E. Speiser, P. P. Lopez-Casas, M. Quintero, A. Ribas, Uncoupling

interferon signaling and antigen presentation to overcome immunotherapy resistance due to JAK1 loss in melanoma. *Sci. Transl. Med.* (2020) doi:10.1126/scitranslmed.abb0152.
18. M. Ayers, J. Lunceford, M. Nebozhyn, E. Murphy, A. Loboda, D. R. Kaufman, A. Albright, J. D. Cheng, S. P. Kang, V. Shankaran, S. A. Piha-Paul, J. Yearley, T. Y. Seiwert, A. Ribas, T. K. McClanahan, IFN-γ-related mRNA profile predicts clinical response to PD-1 blockade. *J. Clin. Invest.* **127**, 2930–2940 (2017).
19. A. Kalbasi, A. Ribas, Tumour-intrinsic resistance to immune checkpoint blockade. *Nat. Rev. Immunol.* **20**, 25–39 (2019).
20. R. H. I. Andtbacka, F. Collichio, K. J. Harrington, M. R. Middleton, G. Downey, K. Öhrling, H. L. Kaufman, Final analyses of OPTiM: A randomized phase III trial of talimogene laherparepvec versus granulocyte-macrophage colony-stimulating factor in unresectable stage III-IV melanoma. *J. Immunother. Cancer* **7**, 145 (2019).
21. A. Ribas, T. Medina, S. Kummar, A. Amin, A. Kalbasi, J. J. Drabick, M. Barve, G. A. Daniels, D. J. Wong, E. V. Schmidt, A. F. Candia, R. L. Coffman, A. C. F. Leung, R. S. Janssen, SD-101 in combination with pembrolizumab in advanced melanoma: Results of a phase 1b, multicenter study. *Cancer Discov.* **8**, 1250–1257 (2018).
22. M. Sade-Feldman, K. Yizhak, S. L. Bjorgaard, J. P. Ray, C. G. de Boer, R. W. Jenkins, D. J. Lieb, J. H. Chen, D. T. Frederick, M. Barzily-Rokni, S. S. Freeman, A. Reuben, P. J. Hoover, A.-C. Villani, E. Ivanova, A. Portell, P. H. Lizotte, A. R. Aref, J.-P. Eliane, M. R. Hammond, H. Vitzthum, S. M. Blackmon, B. Li, V. Gopalakrishnan, S. M. Reddy, Z. A. Cooper, C. P. Paweletz, D. A. Barbie, A. Stemmer-Rachamimov, K. T. Flaherty, J. A. Wargo, G. M. Boland, R. J. Sullivan, G. Getz, N. Hacohen, Defining T cell states associated with response to checkpoint immunotherapy in melanoma. *Cell* **175**, 998–1013.e20 (2018).
23. N. Riaz, J. J. Havel, V. Makarov, A. Desrichard, W. J. Urba, J. S. Sims, F. S. Hodi, S. Martín-Algarra, R. Mandal, W. H. Sharfman, S. Bhatia, W.-J. Hwu, T. F. Gajewski, C. L. Slingluff, D. Chowell, S. M. Kendall, H. Chang, R. Shah, F. Kuo, L. G. T. Morris, J.-W. Sidhom, J. P. Schneck, C. E. Horak, N. Weinhold, T. A. Chan, Tumor and microenvironment evolution during immunotherapy with nivolumab. *Cell* **171**, 934–949.e16 (2017).
24. H. Okamoto, Y. Yoshimatsu, T. Tomizawa, A. Kunita, R. Takayama, T. Morikawa, D. Komura, K. Takahashi, T. Oshima, M. Sato, M. Komai, K. A. Podyma-Inoue, H. Uchida, H. Hamada, K. Fujiu, S. Ishikawa, M. Fukayama, T. Fukuhara, T. Watabe, Interleukin-13 receptor α2 is a novel marker and potential therapeutic target for human melanoma. *Sci. Rep.* **9**, 1281 (2019).
25. J. D. Wolchok, A. Hoos, S. O'Day, J. S. Weber, O. Hamid, C. Lebbé, M. Maio, M. Binder, O. Bohnsack, G. Nichol, R. Humphrey, F. S. Hodi, Guidelines for the evaluation of immune therapy activity in solid tumors: Immune-related response criteria. *Clin. Cancer Res.* **15**, 7412–7420 (2009).
26. J. A. Beaver, M. Hazarika, F. Mulkey, S. Mushti, H. Chen, K. He, R. Sridhara, K. B. Goldberg, M. K. Chuk, D.-C. Chi, J. Chang, A. Barone, S. Balasubramaniam, G. M. Blumenthal, P. Keegan, R. Pazdur, M. R. Theoret, Patients with melanoma treated with an anti-PD-1 antibody beyond RECIST progression: A US Food and Drug Administration pooled analysis. *Lancet Oncol.* **19**, 229–239 (2018).
27. M. Denis, M. Duruisseaux, M. Brevet, C. Dumontet, How can immune checkpoint inhibitors cause hyperprogression in solid tumors? *Front. Immunol.* **11**, 492 (2020).

Acknowledgments: We thank Pivotal as the contract research organization for this clinical trial, and the patients and their families for their generous participation in this study. We also thank A. Kalbasi and A. Ribas from the University of California, Los Angeles (Los Angeles, CA, USA) for their critical review and comments on this work. We also want to thank F. Al-Shahrour, head of the Bioinformatics Unit, Spanish National Cancer Research Center (CNIO), for her valuable advice regarding statistical analysis on gene expression. English style and grammar editing were performed by professional writers at editage.com, financed by the clinical trial sponsor, Highlight Therapeutics (formerly known as Bioncotech Therapeutics). **Funding:** This clinical trial was funded by Bioncotech Therapeutics SL and was partially supported through grants received from CDTI (IDI-20170635) and European Regional Development Funds that were assigned to Bioncotech Therapeutics (currently known as Highlight Therapeutics). **Author contributions:** All the authors read, reviewed, and approved the final version of the manuscript. I.M.-R. and I.M. contributed to the concept, design, patient recruitment, data analysis, and interpretation of the results as well as writing of the manuscript. D.T. and M.Q. contributed to the design of the clinical trial, interpretation of the results, and writing of the manuscript. F.L., M.E.R.-R., A. Calles, J.L.P.-G., A.G.-R., S.L.-T., M.P.-S., R.Á., A.S.-R., M.A.A., A. Calvo, S.P., M.J., B.R.-V., E.C., P.G., E.J.-A., and S.M.-A. contributed to recruiting patients and biological samples. E.d.M. and C.S.-O. contributed with the radiological guided administration of BO-112 to patients and biopsy collection. R.R.-M. and P.P.L.-C. contributed with the translational analysis of patients' samples. **Competing interests:** I.M.-R. has received grants as advisory board member and travel and congress accommodation from BMS, MSD, Roche, Novartis, Amgen, Pierre Fabre, Merck Serono, Sanofi, Regeneron, Incyte, AstraZeneca, and Bioncotech. F.L. has received grants for advisory roles or travel grants from Roche, Merck, Amgen, Sanofi, Lilly, Servier, Bayer, Ferrer, MSD, and BMS. A. Calles has received honorary/consulting fees from AstraZeneca, Boehringer Ingelheim, Pfizer, Roche/Genentech, Eli Lilly and Company, Novartis, Merck Sharp & Dohme, and Bristol-Myers Squibb. J.L.P.-G. has received research grants and support from Roche, BMS, MSD, Ipsen, Eisai, Incyte, and Janssen; speakers bureau and advisory boards fees from Roche, BMS, Ipsen, Eisai, and MSD; and travel support from Roche, MSD, and BMS. S.L.-T. has received grants as a consultant or in advisory roles from Celgene, Novartis, Pierre Fabre, Pfizer, Roche, Eisai, Lilly, and AZ and travel grants from Celgene, Pfizer, Roche, and MSD. M.P.-S. has received grants as advisory board member from AstraZeneca, and travel and congress accommodation from BMS, Roche, Incyte, and Novartis. A. Calvo has received grants for advisory roles and travel grants from MSD, BMS, Merck, Amgen, Sanofi, and Servier. P.P.L.-C. is a full-time Bioncotech Therapeutics SL employee. D.T. is a Bioncotech Therapeutics SL consultant. M.Q. is the chief executive officer of Bioncotech Therapeutics SL and owns stock. M.M. has received research grants from Roche, PUMA, and Novartis; consulting/advisory fees from AstraZeneca, Amgen, Taiho Oncology, Roche/Genentech, Novartis, PharmaMar, Eli Lilly, PUMA, Taiho Oncology, and Pfizer; and speakers' honoraria from AstraZeneca, Amgen, Roche/Genentech, Novartis, Daiichi Sankyo, and Pfizer. I.M. reports receiving commercial research grants from BMS, Alligator, AstraZeneca, and Roche and serves as a consultant/advisory board member for BMS, Merck Serono, Roche-Genentech, Genmab, Incyte, Bioncotech, Tusk, Numab, Molecular Partners, F-star, Alligator, Bayer, and AstraZeneca. Patents: Information related to the manufacturing and medical uses of BO-112 was disclosed in the patent applications published as WO2017/085228 and WO 2018/210439 (M.Q. listed as inventor). Some of the data present in this article have been disclosed in the patent application published as WO2020/104628 (M.Q., D.T., and P.P.L.-C. listed as inventors) (https://patentscope.wipo.int/search/es/detail.jsf?docId=WO2020104628&tab=PCTBIBLIO&_cid=P10-KDOCU7-14730-1). All other authors declare that they have no competing interests. **Data and materials availability:** All data associated with this study are present in the paper or in the Supplementary Materials.

Submitted 24 January 2020
Accepted 13 August 2020
Published 14 October 2020
10.1126/scitranslmed.abb0391

Citation: I. Márquez-Rodas, F. Longo, M. E. Rodriguez-Ruiz, A. Calles, S. Ponce, M. Jove, B. Rubio-Viqueira, J. L. Perez-Gracia, A. Gómez-Rueda, S. López-Tarruella, M. Ponz-Sarvise, R. Álvarez, A. Soria-Rivas, E. de Miguel, R. Ramos-Medina, E. Castañon, P. Gajate, C. Sempere-Ortega, E. Jiménez-Aguilar, M. A. Aznar, A. Calvo, P. P. Lopez-Casas, S. Martín-Algarra, M. Martín, D. Tersago, M. Quintero, I. Melero, Intratumoral nanoplexed poly I:C BO-112 in combination with systemic anti–PD-1 for patients with anti–PD-1–refractory tumors. *Sci. Transl. Med.* **12**, eabb0391 (2020).

Science Translational Medicine

Intratumoral nanoplexed poly I:C BO-112 in combination with systemic anti–PD-1 for patients with anti–PD-1–refractory tumors

Iván Márquez-Rodas, Federico Longo, Maria E. Rodriguez-Ruiz, Antonio Calles, Santiago Ponce, Maria Jove, Belén Rubio-Viqueira, Jose Luis Perez-Gracia, Ana Gómez-Rueda, Sara López-Tarruella, Mariano Ponz-Sarvise, Rosa Álvarez, Ainara Soria-Rivas, Enrique de Miguel, Rocío Ramos-Medina, Eduardo Castañon, Pablo Gajate, Cayetano Sempere-Ortega, Elisabeth Jiménez-Aguilar, M. Angela Aznar, Aitana Calvo, Pedro P. Lopez-Casas, Salvador Martín-Algarra, Miguel Martín, Dominique Tersago, Marisol Quintero and Ignacio Melero

Sci Transl Med **12**, eabb0391.
DOI: 10.1126/scitranslmed.abb0391

Interfering with cancer

Many immunotherapies for cancer have emerged in recent years, but none are universally effective. One potential problem is the loss of interferon signaling in tumors, which impairs the effectiveness of both immune checkpoint blockade and cell-based therapies. Kalbasi *et al*. determined that both JAK1 and JAK2 signaling were essential for the success of immune checkpoint blockade, whereas cell-based therapy only required JAK1 function, which maintained sufficient interferon signaling. The authors showed that defective interferon signaling in tumors could be bypassed with the immunostimulatory compound BO-112. In a companion clinical trial, Márquez-Rodas *et al*. tested BO-112 in human patients with cancer, with or without immune checkpoint blockade.

Science Translational Medicine (ISSN 1946-6242) is published by the American Association for the Advancement of Science, 1200 New York Avenue NW, Washington, DC 20005. The title *Science Translational Medicine* is a registered trademark of AAAS.